The experimental plan of displacement- and frequency-noise free laser interferometer

K. Kokeyama[1], S. Sato[2], A. Nishizawa[3], S. Kawamura[2], Y. Chen[4], R. L. Ward[5], A. Pai[4], K. Somiya[4] and A. Sugamoto[6]

[1] Graduate School of Humanities and Sciences, Ochanomizu University, 2-1-1, Otsuka, Bunkyo-ku, Tokyo, 112-8610 Japan
[2] TAMA Project, National Astronomical Observatory of Japan, 2-21-1, Osawa, Mitaka, Tokyo 181-8588 Japan
[3] Graduate School of Human and Environmental Studies, Kyoto University, Kyoto 606-8501, Japan
[4] Max-Planck-Institut für Gravitationsphysik, Am Mühlenberg 1, 14476 Potsdam, Germany
[5] LIGO Project 18-34, California Institute of Technology, Pasadena, California 91125, USA
[6] Ochanomizu University, 2-1-1, Otsuka, Bunkyo-ku, Tokyo, 112-8610 Japan

E-mail: keiko.kokeyama@nao.ac.jp

Abstract. We present the partial demonstration of displacement- and laser-noise free interferometer (DFI) and the next experimental plan to examine the complete configuration. A part of the full implement of DFI has been demonstrated to confirm the cancellation of beamsplitter displacements. The displacements were suppressed about two orders of magnitude. The aim of the next experiment is to operate the system and to confirm the cancellation of all displacement noises, while the gravitational wave (GW) signals survive. The optical displacements will be simulated by Electro-optic modulators (EOM). To simulate the GW contribution to laser lights, we will use multiple EOMs.

1. Introduction

Gravitational waves (GW) have been searched for years by ground-based GW detectors [1-6]. However, they have not been detected yet since their amplitudes are quite tiny and the detectors are disturbed by a great amount of noise. The sensitivities of the detectors are limited by various noises, e.g., seismic- and gravity gradient disturbances, thermal noises in mirrors and suspensions, and shot noises. Recently, theoretical investigation of the GW detectors which are free from both the displacement noise of the optics and the laser frequency noises are newly proposed [7, 8]. In these two papers, it was shown that when an N-test-mass array ($N > d+2, d$ is the dimension of test masses) consists multiple interferometers, one can make a signal combination which does not sense displacement- and frequency-noises but sense the GW contribution. It is carried out by the fact that the GW contribution to phase shifts of laser lightd takes a form different from that of optics displacements.

In the next section, we introduce the DFI configuration suggested in [9]. In section 3 The result of proof-of-principle experiment is presented. The experimental plan of the next experiment will be explained in section 4.

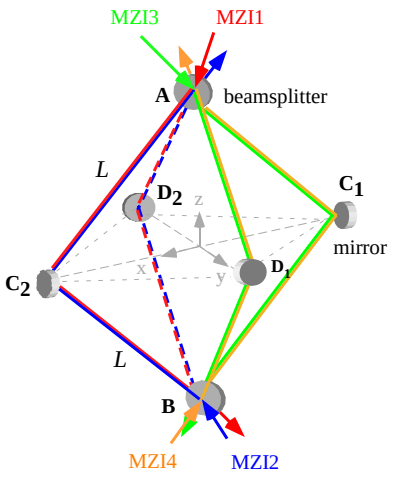

Figure 1. The 3-D DFI configuration. It consists of 4 Mach-Zehnder interferometers, MZI1, MZI2, MZI3 and MZI4. A and B are beamsplitters, and $C_{1,2}$ and $D_{1,2}$ are steering mirrors. Path lengths between mirrors and beamsplitters are L. The light path of MZI1 is $A_tD_2B_r$ - $A_rC_2B_t$; MZI2 is $B_tD_2A_r$ - $B_rC_2A_t$; MZI3 is $A_tC_1B_r$-$A_rD_1B_t$; MZI4 is $B_tC_1A_r$ -$B_rD_1A_t$;. The subscripts r and t denote reflection and transmission at the beamsplitters.

2. DFI configuration

Reference [9] proposed 2D and 3D optical designs of DFI implemented by four Mach-Zehnder interferometers (MZI). Figure 1 shows the 3D design that we are going to construct. In this configuration, there are four MZIs on an octahedron path. The arm lengths of MZIs are equal so that the frequency noises are canceled by each interferometer itself. There are two MZIs, counterpropagating on the same optical path (which is called bidirectional MZI) so that the displacements of the two folding mirrors are detected redundantly. The displacements can be eliminated clearly from by combining the two signals. To eliminate the beamsplitter displacements, an additional pair of bidirectional MZI is employed. Thus two bidirectional MZIs sense the two beamsplitters redundantly and the displacement noises can be removed. The GW signals will remain in the combined signals because the GW and displacement noises contribute to light propagation in different manners. As discussed in [9], the DFI signal has the sensitivity to GWs at low frequencies is proportional to $(\Omega_{\rm GW}L/c)^2$ for 3D configuration, where $\Omega_{\rm GW}$ is the GW frequency.

3. Partial demonstration

So far, the bidirectional MZI has already demonstrated. The displacement noises of the folding mirrors were simulated by EOMs and the suppression of about 45 dB was attained [10, 11]. As a next step, the cancellation of beamsplitter motion has been examined. We actually actuated the beamsplitter, and confirmed the cancellation of the displacement-noise signals.

3.1. Experiment

Figure 2 shows the optical layout of the experiment. Four mirrors and two beamsplitters compose two MZIs which share the beamsplitters. These interferometers correspond to the combination of MZI1 and MZI3 in Fig. 1 although they are *squished* to 2D. In this 2D configuration, the two input beams go into the interferometer. The incident beams are firstly separated by beamsplitter A, then propagate the inline and perpendicular arms. Here, we defined that the inline arm is the path transmitting A and the perpendicular arm is the path reflected by A. The two beams interfere after the second beamsplitter, B. There are two output ports which correspond to e.g. a bright port and a dark port of Michelson interferometer. The laser fields are detected by the photo detectors, PD1 and PD3 for MZI1 and MZI3 respectively. One of the output signals is to control to give a mid-fringe locking. The other signals are to monitor the beamsplitter displacements. The PZT (piezoelectric transducer) is attached to the beamsplitter-holder to

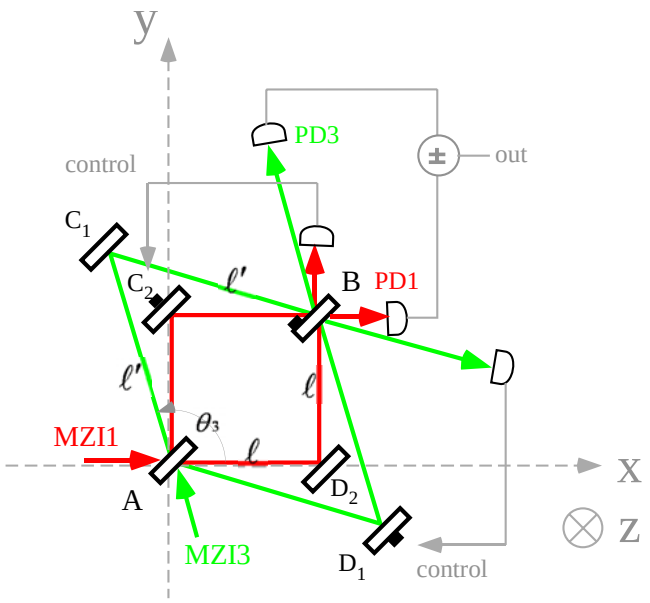

Figure 2. The setup for the proof-of-principle experiment. Two symmetrical MZIs share two beamsplitters. The beamsplitter at the output port are shaken by an attached PZT. The displacement is sensed by the two MZIs redundantly. The two outputs (out1 and out3 for MZI1 and MZI3) are electrically subtracted. so that the beamsplitter displacement signals are suppressed. ℓ and ℓ' denote the length between a beamsplitter and a mirror of MZI1 and MZI3 respectively. The inline arm of MZI1 is parallel to the x axis. The inline arm of MZI3 inclines to the x axis at an angle θ_3 ($\pi/4 < \theta_3 < 3\pi/4$).

simulate displacement noises. The output signals of MZI1 and MZI3 (out1 and out3 respectevely) are sent to a electric subtracter to cancel the displacement noises.

When beamsplitter B is excited by the attached PZT at an angular frequency ω and an amplitude $d\ell_0$, the paths length are changed. In addition, we suppose the + polarized GWs are coming along the z direction. The output signals of PD1 and PD3 with the GW effect can be respectively written as,

$$V_{\rm PD1}(\omega) \propto \frac{\Omega_0 d\ell_1}{c} + \frac{\Omega_0}{\omega}\sin\frac{\ell\omega}{c}e^{-i\ell\omega/c} \quad (1)$$

$$V_{\rm PD3}(\omega) \propto \frac{\Omega_0 d\ell_3}{c} + \frac{\Omega_0}{\omega}(\cos^2\theta_3 - \sin^2\theta_3)\sin\frac{\ell'\omega}{c}e^{-i\ell'\omega/c} \quad (2)$$

where $d\ell_1 = \sqrt{2}d\ell_0$ and $d\ell_3 = \frac{1-\cos(2\theta_3)}{\cos(3\pi/4-\theta_3)}d\ell_0$ which are caused by the inclines to the beamsplitter. The second terms of Eq. (1) and (2) are the effects caused by the GWs. Subtracting the two signals with an appropriate gain adjustment, we can remove the displacement-noise signals, while the GW signals are retaining.

However, in this table-top experiment, little GW signal surviving is expected since we saw the signal only from DC to 1kHz region. A PZT can excite the beamsplitter only below 1kHz. GW signals survive around a few hundred MHz for the table-top interferometers of this scale (ℓ was $\sim$0.3m).

3.2. Result

Figure 3 shows the result of the displacement-noise suppression. The plots are the magnitude and phase of the transfer functions from the beamsplitter to out1, out3, and the subtracted signal respectively, including the response functions of the PZT and the photo detectors. The magnitude of out1 and out3 were tuned appropriately so that the displacement-noise signals disappeared. About two orders of suppression was achieved in a frequency region in which the PZT can be excited flatly. Many mechanical resonants due to the PZT, and ones caused by coupling of the PZT and the beamsplitter were seen above 1 kHZ. In this region, the displacement-noise were not canceled owing to the different MZI responses to the beamsplitter motion.

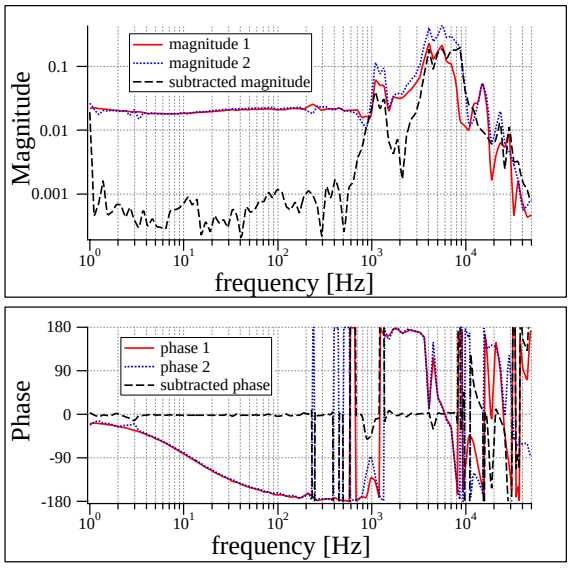

Figure 3. Magnitude and phases of the transfer function from beamsplitter displacements to output signals. Solid-red and dashed-blue plots are magnitudes of the transfer function from the beamsplitter to PD1 and PD3 respectively, giving almost same response below about 1 kHz. Dotted-black lines are magnitude and phase of the DFI signal. Approximately two orders of magnitude of suppression can be seen from DC to 1 kHz. The suppression depends on subtle adjustments of the balance between the two outputs.

4. Experimental Plan for 3D Full Configuration

In our next experiment, the DFI will be constructed in 3D space and operated in the full configuration just as shown in Fig. 2. The signals of the four MZIs will be extracted and combined so that displacement noises disappear. The output voltage of each interferometer can be written in frequency domain

$$V_1(\omega) \propto dx(C_2)\frac{\Omega_0}{c}e^{i\omega L/c} + dx(D_2)\frac{\Omega_0}{c}e^{i\omega L/c} + dx(A)\frac{\Omega_0}{c}e^{2i\omega L/c} + dx(B) \quad (3)$$

$$V_2(\omega) \propto dx(C_2)\frac{\Omega_0}{c}e^{i\omega L/c} + dx(D_2)\frac{\Omega_0}{c}e^{i\omega L/c} + dx(A) + dx(B)\frac{\Omega_0}{c}e^{2i\omega L/c} \quad (4)$$

$$V_3(\omega) \propto dx(C_1)\frac{\Omega_0}{c}e^{i\omega L/c} + dx(D_1)\frac{\Omega_0}{c}e^{i\omega L/c} + dx(A)\frac{\Omega_0}{c}e^{2i\omega L/c} + dx(B) \quad (5)$$

$$V_4(\omega) \propto dx(C_1)\frac{\Omega_0}{c}e^{i\omega L/c} + dx(D_1)\frac{\Omega_0}{c}e^{i\omega L/c} + dx(A) + dx(B)\frac{\Omega_0}{c}e^{2i\omega L/c} \quad (6)$$

where $dx(C_1), dx(C_2)\cdots$ are the amplitudes of the displacement of C_1, C_2 and so on. Using electric subtracters, we will obtain the DFI signal $V_{\rm DFI}(\omega)$, by combining the signals;

$$V_{\rm DFI}(\omega) = (V_1(\omega) - V_2(\omega)) - (V_3(\omega) - V_4(\omega)). \quad (7)$$

As was given by Eq. (16) in [9], when the + polarized GWs come along the z direction, the DFI signal will respond to the GWs in such a way that

$$H_{\rm GW} = \frac{i\Omega_0 h e^{i2\omega L/c}}{4\omega}\Big[(2-\sqrt{2})[1-e^{(4+2\sqrt{2})i\omega L/c}] + (2+\sqrt{2})[e^{4i\omega L/c} - e^{2\sqrt{2}i\omega L/c}]\Big]. \quad (8)$$

Figure 4 shows the plot of the response when the arm length L=0.4m. The peak frequency depends on L. In this case, GW signals retain around approximately 200 MHz. Below the peak frequency, the response is attenuated in proportional to f^2. Practically there are merely little displacement noises such a high frequency region. However the observation range can become lower for a larger size of DFI. Such DFIs with long arms are very effective since in lower frequency displacement noises limit the sensitivity.

We will confirm that all test-mass displacements are canceled while GW signals are retained in the DFI signals. To confirm the cancellation, mirror displacements, beamsplitter displacements, and GW effects should be simulated.

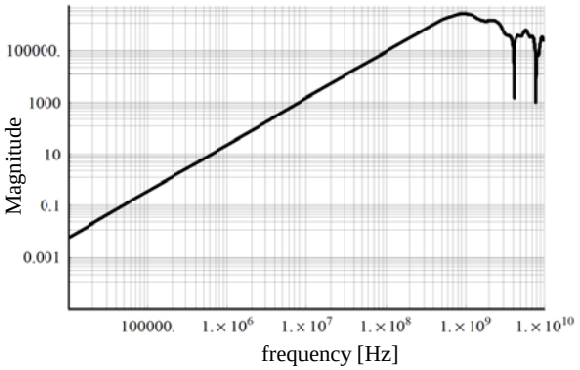

Figure 4. Transfer function from the GW to the DFI signal when $L =$ 0.4 m. The peak frequency depends on the length L. In our experiment, GW signals are expected around 200 MHz. The GW effects will be simulated by using multiple EOMs.

4.1. Optic-displacements simulator

The mirror noises are injected by EOMs in the same way as the previous proof-of-principle experiment shown in [10]. For example, when the displacements of beamsplitter D_2 are simulated, we put an EOM (E1) at the middle point of the path.

The method to simulate beamsplitter noises is different from the one explained in section 3 in the two points, the simulator and configuration. First, EOM will be employed as a displacement simulator to observe the cancellation in broader frequency region where the survived-GW signals can be seen. Second, the configuration will be in 3D space, being shown in Fig. 1. To simulate this, two identical EOMs are put on perpendicular paths of MZI1 and MZI2 respectively. Although there must be four identical EOMs to mimic the beamsplitter displacements naively, the two EOMs will be applied on the two optical paths because of the fact that actuating two lengths differentially and actuating one length of the two are similar effects. The two EOMs will be put on a paths just next to A.

4.2. GW simulator

The GWs affects not only one point on the laser path but the whole path. Therefore putting an EOM on a laser path can not simulate such effects because it yields phase changes at only one point where it is putting on. A straight forward way to simulate the real GW effects is to fill EOMs the whole laser paths. However, such many EOMs covering laser paths will cause the serious reduction of interferometer contrast. Therefore we adopt a tricky procedure. First, we will put an EOM at one point and take data then put the EOM at the next point and take data. Repeating this procedure and summing them, we will be able to duplicate the GW effect on the laser path.

5. Conclusions

In this paper we have presented the demonstration of the partially implemented DFI. The noise suppression of about two orders of magnitude was achieved. The displacement noise of a beamsplitter was injected by the attached PZT. In addition, the next experimental plan has been presented. The DFI in the 3D configuration will be built and operated. The GW-signal survival will be confirmed around 200 MHz while all the optical displacements are canceled in the DFI signals. The optic displacements will be simulated by EOMs.

Acknowledgments

The authors gratefully acknowledge the support of the research Japan Society for the Promotion of Science and Grant-in-Aid for Scientific Research. The authors also gratefully acknowledge the support of the United States National Science Foundation for the construction and operation

of the LIGO Laboratory and the Science and Technology Facilities Council of the United Kingdom, the Max-Planck-Society, and the State of Niedersachsen/ Germany for support of the construction and operation of the GEO600 detector.

References

[1] A. Abramovici *et al.*, Science **256**, 325 (1992)
[2] D. Sigg *et al.*, Class. Quantum Grav. **23**, S51 (2006)
[3] F. Acernese *et al.*, Class. Quantum Grav. **23**, S635 (2006)
[4] H. Lück *et al.*, Class. Quantum Grav. **23**, S71 (2006)
[5] M. Ando *et al.*, Class. Quantum Grav. **22**, S881 (2006)
[6] D. E. McClelland *et al.*, Class. Quantum Grav. **23**, S41 (2006)
[7] S. Kawamura and Y. Chen, 2004 *Phys. Rev. Lett.* **93** 211103
[8] Y. Chen and S. Kawamura, 2006 *Phys. Rev. Lett.* **96** 231102
[9] Y. Chen *et al*, 2006 *Phys. Rev. Lett.* **97** 151103
[10] S. Sato *et al*, 2007 *Phys. Rev. Lett.* **98** 141101
[11] S. Sato *et al*, in this volume